Slow polarization relaxation in non-uniform telluric acid ammonium phosphate crystals

2006 J. Phys.: Condens. Matter 18 7687

(http://iopscience.iop.org/0953-8984/18/32/016)

INSTITUTE OF PHYSICS PUBLISHING JOURNAL OF PHYSICS: CONDENSED MATTER

J. Phys.: Condens. Matter **18** (2006) 7687–7701 doi:10.1088/0953-8984/18/32/016

Slow polarization relaxation in non-uniform telluric acid ammonium phosphate crystals

K Matyjasek and R Z Rogowski

Institute of Physics, Szczecin University of Technology, Aleja Piastow 48 70-311 Szczecin, Poland

Received 21 April 2006, in final form 28 June 2006
Published 31 July 2006
Online at stacks.iop.org/JPhysCM/18/7687

Abstract

The characteristic features of polarization and spontaneous depolarization kinetics in non-uniform telluric acid ammonium phosphate (TAAP) crystals are investigated by observation of the domain structure using a nematic liquid crystal method. We present experimental results showing the correlation between the internal bias field, responsible for the offset of the hysteresis loop and the backswitching process. The internal field caused by structural disorder accounts for a broad spectrum of energy barriers for domain nucleation. The switching kinetics was analysed in the framework of the nucleation and growth model based on Avrami statistical theory, using the modified Kolmogorov–Avrami–Ishibashi (KAI) model. It has been found that the switching kinetics in TAAP crystals can be approximated by averaging the KAI model over a broad distribution of characteristic domain growth times. The spectra of the distribution of the characteristic domain growth times are derived from the experimental data.

1. Introduction

The mechanism of polarization switching in ferroelectric materials has been intensively discussed in recent years, in association with the recent development of memory devices [1]. Polarization switching, which proceeds by nucleation and growth of domains, has attracted much attention also from the viewpoint of statistical physics related to solid-state transformation. Random nucleation and isotropic growth of ferroelectric domains is well described by using the Kolmogorov–Avrami–Ishibashi (KAI) model, which is based on the classical approach of nucleation and growth kinetics [2]. This model has been used to fit data fairly well in many single crystals [3, 4], and polycrystalline and epitaxial films [5, 6]. However, the data analysis has revealed no integer dimensionality of the domain growth, contrary to the Avrami equation, which is restricted to integer values. Kikuta *et al* [7] applied the KAI model to analyse the switching current data in TAAP crystals. The effective dimensionality of the domain growth has proved to be not integer, and is dependent on the temperature and electric field. Recently, several attempts have been made to solve the finite-size problem [8, 9]. The effects due to finite sizes are very important in polycrystalline films

and ceramics, as in such materials the domain structure is simultaneously and independently reconstructed in small grains. The KAI model has as its rate-limiting parameter the domain wall speed. Recently, it has been found that over a very wide range of electric fields, the KAI model is not a good description of switching process and that a nucleation-limited model is more appropriate [10, 11]. In the Tagantsev approach [11] a number of non-interacting elementary switching regions are considered. Switching kinetics was described in terms of the distribution function of nucleation probabilities in these regions. In our earlier report [12], a similar approach has been proposed for describing the switching kinetics in non-uniform $(CH_3NH_3)_5Bi_2Br_{11}$ single crystals, in which the domain walls and their motion are decisive for the polarization switching. The switching kinetics was described based on a modified KAI model, assuming a statistical distribution of characteristic domain growth times. In this report we perform a test of validity of the modified KAI model for non-uniform telluric acid ammonium phosphate (TAAP) single crystals.

In contrast to polarization switching in an electric field, comparatively less has been reported on the mechanism that controls the spontaneous reversal of polarization, which occurs in the absence of an external electric field [13, 14]. The phenomenon of time-dependent polarization loss (retention failure) in poled ferroelectrics is a major problem in ferroelectric non-volatile memories. Therefore, disclosing the nature of the depolarization mechanism remains of particular scientific and technological interest. The polarization relaxation that occurs in the absence of an electric field is driven primarily by a depolarization field present due to charge redistribution near the electrode–thin-film interface [15–17], and an internal field that has been attributed to dipolar defects in the bulk of the crystal [18–20]. Optical techniques are much more valuable in obtaining spatio-temporal information about polarization switching and are a useful complement to the usual electric measurements. Recently a nanoscale mechanism of polarization relaxation in thin films has been intensively investigated by means of piezoresponse scanning force microscopy [15, 16, 21]. In this report direct observation of the evolution of the domain structure during polarization reversal was performed by the nematic liquid crystal (NLC) decoration technique. This method enables one to observe directly the single domains (up to 1 μm in size) and the entire surface of the sample during polarization reversal. This paper reports a comprehensive study of the switching kinetics in non-uniform TAAP crystals. We discuss the investigations on the temporal behaviour of the polarization in dc electric fields as well as polarization decay after removal of the electric field.

2. Experimental details

TAAP, having a chemical formula $Te(OH)_6{\cdot}2NH_4H_2PO_4{\cdot}(NH_4)_2HPO_4$, undergoes a phase transition at $\sim$321 K, changing its symmetry from the centrosymmetric class 2/*m* to the polar class *m* [22]. It is an order–disorder transition involving proton motion with hydrogen bonds [23, 24]. The crystals were grown from an aqueous solution at room temperature. Two telluric acid ammonium phosphates are crystallized from an aqueous solution of ammonium hydroxide, telluric acid and phosphoric acid at room temperature [25]; triclinic crystal $Te(OH)_6{\cdot}2(NH_4)_2HPO_4$ and monoclinic TAAP. Only the monoclinic crystal is ferroelectric. The large and more homogeneous TAAP single crystals were obtained from non-stoichiometric solution rich in $(NH_4)_2HPO_4$. The composition of the solution was the same as described by Nicolau [25]. The aqueous solutions of telluric acid, ammonium dihydrogen phosphate and diammonium hydrogen phosphate were mixed in the required proportions as to obtain the atom ratios N:P:Te of 6:4:1.

To observe optically indistinguishable 180° domain walls, the nematic liquid crystal (NLC) decoration technique was used [26]. The NLC mixture of p-methoxybenzylidene-

p-n-butylaniline (MBBA) and p-ethoxybenzylidene-p-n-butylaniline (EBBA) was used. For dynamic observation in an electric field a crystal plate with a thin NLC layer, on its upper and lower face, was sandwiched between two glass plates with thin oxide coating as transparent electrodes. Observation of domain structure dynamics was made on the (101) natural face of the crystal, which is approximately normal to the spontaneous polarization direction. The domains were observed using a polarization microscope and recorded with a digital camera. The recorded domain patterns were analysed using the image processing programme. The hysteresis loop was obtained by means of a modified Sawyer–Tower bridge using an ac electric field of 50 Hz. An air-drying silver paste was used as electrodes.

3. Results and discussion

Microscopic observations of the domain structure show that TAAP crystals are highly inhomogeneous; regions may exist that exhibit switchable polarization and there are parts with more fixed polarization. Hence, we can cut out large samples that reveal unipolar characteristics. The results presented here refer to a single sample of TAAP crystal with surface area of 0.18 cm^2 and thickness 0.05 cm (in the polarization direction). However, these results are typical of a fairly large number of specimens that reveal initial static unipolarity not removed during the annealing of the crystal above the Curie temperature. Annealing lowers the threshold nucleation field, increases the number of nuclei active in an electric field, and enhances the dynamic mobility of the domain walls. In freshly annealed crystal samples the switching parameters changed with the elapse of time. The experiments were carried out a few days after annealing of the sample, so that the domain structure was more stable and the domain structure, in the electric field, changed nearly reproducibly by repeated experiments in the same conditions. Prior to the measurements the sample was electrically deaged by using a bipolar rectangular pulse train ($\pm$400 kV m^{-1} 1 Hz, 100 pulses). In the electrically deaged samples the domain pinning centres were removed, and the domain walls follow the external field freely, leading to a monodomain state in the crystal.

The main characteristic of a ferroelectric is its hysteresis loop, obtained when the sample is switched from one saturated state of polarization to another with an applied electric field. Figure 1 shows the hysteresis loop of the sample used in this study. The large asymmetry of the hysteresis loop about the electric field axis indicates the presence of an internal bias field, E_b, defined as a shift of the hysteresis loop on the electric field axis. Direct imaging of the domain configuration revealed that this is a result of a preference of one polarization state over another in ferroelectric bistability. For convenience, the polarization state will be denoted as positive or negative depending on the voltage direction. If polarization vector is directed from bottom to top electrode, it will be referred to as the positive state. The examined crystal sample was in a single domain state with negative polarization, because polarization reversal took place by applying an external positive dc field. After switching the polarization vector under an external electric field an unstable state of polarization is created, which then relaxes to nearly the initial single domain state. The images presented in figure 2 were taken on the large surface area ($\sim$12 mm^2) of the sample during the switching process in $E = 220$ kV m^{-1} (figures 2(a), (b)) and spontaneous backswitching process after removal of the poling field (figures 2(c), (d)). The polarization axis is approximately normal to the image plane. In both cases, the switching from one single-domain state to another is realized by the nucleation and growth of domains. It must be noted that in more homogeneous crystal samples with a small asymmetry of the switching process (with a non-basic or slightly biased hysteresis loop with respect to the origin), the newly created domains are mostly stable after removal of the poling field. In the examined crystal sample in which the magnitude of E_b (225 kV m^{-1}, estimated as a biased field of the hysteresis

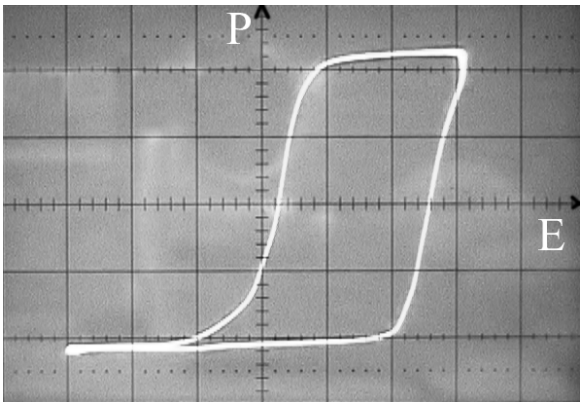

Figure 1. The polarization hysteresis loop of unipolar TAAP crystal. The vertical scale is 0.5 μC cm^{-2} per large division and the horizontal scale is 160 kV m^{-1} per large division.

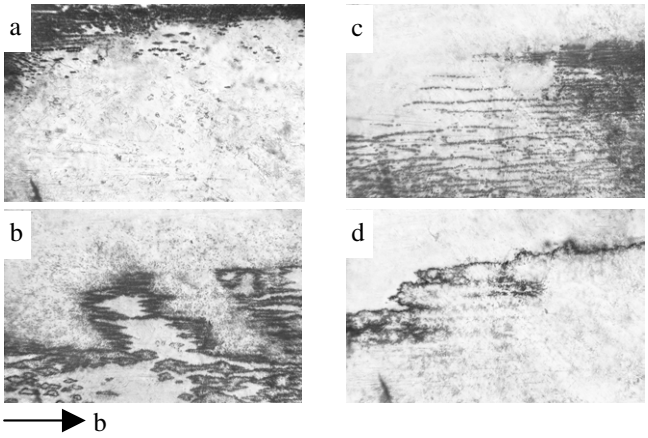

Figure 2. Sequence of photographs showing domain pattern evolution observed on the (101) plane of the TAAP crystal (surface area ∼0.12 cm^2) during the switching process in an electric field of 220 kV m^{-1} ((a), (b)) and spontaneous backswitching process after removal of the electric field ((c), (d)). The electric field was removed when the switching process was completed in the crystal sample. The polarization axis is approximately normal to the image plane (101).

loop) exceeds the coercive field (190 kV m^{-1}, defined as the half width of the hysteresis loop), the spontaneous backswitching process occurs when the external poling field returns to zero.

The value of E_b estimated from the hysteresis loop is the average field in the whole crystal sample (surface area of 18 mm^2). In the imaging area, as shown in figure 2 (12 mm^2), the external field that must be applied to reverse the direction of polarization is lower than the average E_b. The local internal field can be estimated, similarly, as a bias field of the hysteresis loop, as $E_\mathrm{b} = 0.5(E_\mathrm{c}^\mathrm{s} + E_\mathrm{c}^\mathrm{b})$, where E_c^s and E_c^b are the lowest fields needed to reverse the direction of polarization for switching and backswitching processes, respectively. The local internal field obtained in the same small surface area but located in various regions of TAAP crystal sample can differ from that obtained from the hysteresis loop by ∼40%.

The method for studying the domain kinetics is based on the visualization with NLC of the moving domain walls. The reversed regions, where reorientation of the domain structure

still occurs, look somewhat darker than the 'white' surrounding domains, as in these regions a certain electrohydrodynamic instability, particularly dynamic scattering of NLC molecules, takes place [26]. It should be emphasized that the thickness of the 'visible' walls is not the real physical thickness of the domain walls, which are usually very thin, of the order of a few lattice constants.

As was described in detail in [27], the domain configuration arising during polarization reversal in TAAP crystal depends greatly on the electric field strength applied to the crystal. In weak dc fields plate-like domains elongated in the b-direction were observed on the crystal surface normal to the polar axis. In higher electric fields circular domains are nucleated, but anisotropy of the domain wall motion results in elliptical shape domains. In large electric fields the domain nuclei are not distributed randomly on the crystal surface, but are arranged in rows oriented parallel to the b-direction. With increasing field the density of the domain nuclei in each row and the number of rows per unit length increase, so they become optically indistinguishable. Simultaneous formation of nuclei in each row may be thought of as a result of approximately equal activation energy of nucleation in a given row. This indicates the importance of crystallographic factors in the ordering of the defects in the process of crystal growth. Similar ordered alignment of domain nuclei, and thus of defect sites which are nucleation centres, was also induced in a thermal shock. Stripe-like domains elongated in the b-direction have been observed in an as-grown crystal sample that exhibits only a small initial unipolarity [27].

The inhomogeneous distribution of the domain nuclei during switching and spontaneous backswitching processes (see figures 2(a) and (c) respectively) is a result of non-uniform internal field distribution. Defects play the active role of charged centres in the formation of a new phase [28]. This means that a number of regions may have a different defect concentration. Although it is difficult to determine the precise distribution of internal field within the crystal sample experimentally, one can deduce it from the distribution of the domain nuclei induced by E_b (under no external field). The density of rows (in which nuclei are arranged) per unit length gradually diminishes from the lower to the upper part of the image in figure 2(c), demonstrating that E_b has progressively smaller values. The backswitching process occurs very quickly (on the time scale of milliseconds) in the lower part of the image and more slowly (on the time scale of seconds) in the upper part of the image, where the spontaneous backswitching process proceeds through the motion of the domain wall front (see figure 2(d)). This progressive decrease of E_b within the crystal sample is also apparent during the switching process in an electric field; first nucleation of domains, arranged in rows, is observed in the upper region of the image in figure 2(a) and elliptical shape domains arise in the lower part of the image. Such changes in the domain configurations result from inhomogeneities in the internal field distribution that influence the rate of nucleation and domain growth at a given site of a crystal. The effective field is comprised of the sum of the applied external electric field, a depolarization field due to the unscreened portion of the polarization bound charges, and an internal field E_b, which has been attributed to the defects in the bulk of the crystal.

In ferroelectric materials with conducting electrodes the depolarization field is screened in part by the fast redistribution of charges at the electrodes accompanying the current in the external circuit (external screening) [28]. However, if a thin low conducting NLC layer exists at the interface between the electrode and the ferroelectric, this can give rise to a residual depolarization field in the interior of the ferroelectric crystal. The fact that the spontaneous backswitching process has not been observed in homogeneous crystal samples (with a symmetrical hysteresis loop about the P and E axes) demonstrates that the polarization relaxation behaviour should be dominated by directional internal field E_b, caused by structural disorder in the examined TAAP crystal sample.

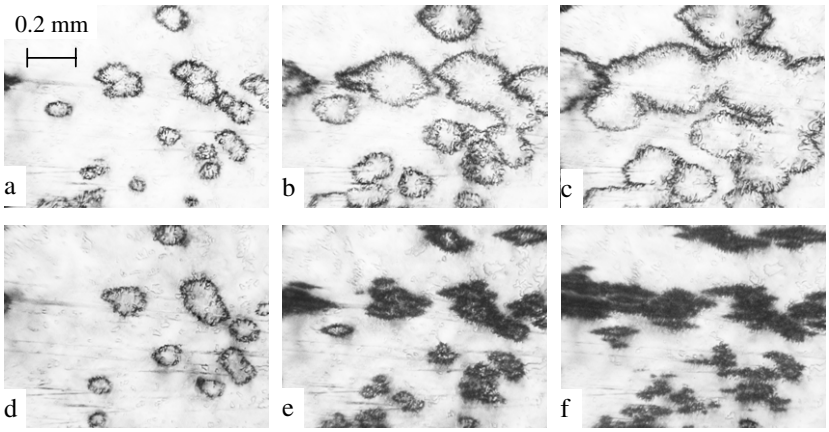

Figure 3. Selected video frames in recording of domain pattern evolution during the switching process in $E = 240$ kV m^{-1} (a)–(c). Time from the moment of applying the electric field: (a) 0.8 s, (b) 1.6 s, (c) 2.4 s. Distribution of domains in three various electric fields, observed on the small surface area ($\sim$1 mm^2) of the crystal: (d) 220 kV m^{-1}, (e) 260 kV m^{-1}, (f) 280 kV m^{-1}. Time from the moment of applying electric field: (d) 1 s, (e) 0.4 s, (f) 0.2 s.

Microscopic observation enables us to investigate the kinetics of the switching process in a small region of the crystal sample to assure compositional homogeneity, with spatially random position of nucleation sites (the main assumption in the KAI model), as well as in a highly inhomogeneous region, with a spatially non-uniform distribution of domain nuclei. Recording of the domain patterns was performed under video control with a 40 ms resolution clock.

3.1. Kinetics of the switching process in a region with spatially uniform distribution of domain nuclei over the crystal surface

Figures 3(a)–(c) show the series of video frames illustrating the domain pattern evolution observed in a small (about 1 mm^2) fragment of the crystal sample, located in the lower left-hand part of the image in figure 2. In this region elliptical shape domains, randomly distributed over the crystal surface, are observed in a dc field of 240 kV m^{-1}. The defects locally affect the sidewise motion of the domain walls, which manifests itself by the irregular shape of the domain walls. The experimentally observed fluctuations of the single domain wall velocity by two orders of magnitude are indicative of a broad distribution of the wall mobility. A single-domain wall moves at $E = 240$ kV m^{-1} with a mean velocity of $\sim 7 \times 10^{-5}$ m s^{-1} along the crystallographic b-direction and $\sim 2 \times 10^{-5}$ m s^{-1} perpendicularly to the b-direction. A variation in the mean wall velocity from domain to domain by a factor $\sim$3 was observed. In higher dc fields the density of the domain nuclei increases, and domain distribution over the crystal surface becomes more inhomogeneous (as shown in figure 3(f)). It is difficult to monitor the spontaneous backswitching process in this region, due to a rapid relaxation of the reversed polarization to the initial state, which proceeds by nucleation and growth of backswitching domains arranged in regular rows.

Optical microscopy inspection, on opposite polar faces, showed complete penetration of the domains throughout the crystal bulk. This means that the forward domain growth, along the polarization direction, occurs very quickly, and sidewise domain growth determines the kinetics of polarization reversal. Thus, the domain growth becomes a two-dimensional problem. The kinetics of polarization relaxation was determined by measuring the fraction of the switched

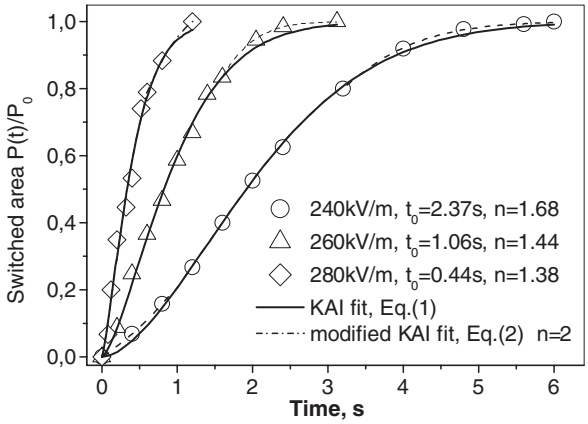

Figure 4. Time dependence of the switched area for various electric fields calculated for domain configurations as shown in figure 3.

area as a function of time as domain structure is naturally linked to the polarization state of the crystal.

3.1.1. Analysis of switching process in the framework of the modified KAI model. In the standard KAI model, the volume fraction of the switched domains to the total volume is given by a simple formula

$$P(t)/P_0 = 1 - \exp(-t/t_0)^n \tag{1}$$

where t is the time since application of an electric field and t_0 is a characteristic domain growth time. The exponent n depends on the spatial dimensionality of the domain growth d (which can take integer values of 1, 2, 3) and the mechanism of nucleation. Equation (1) refers to heterogeneous nucleation, that occurs in the vicinity of defects; thus the effective dimensionality is $n = d$. In homogeneous nucleation the nuclei continue to occur at a constant rate during switching; thus $n = d + 1$. The KAI model is a simplification of the real physical conditions assuming a spatial uniform nucleation probability and a constant domain growth velocity.

Figure 4 plots the fraction of the switched area as a function of time, for the domain configuration as shown in figure 3. The function equation (1) (full curves) agrees well with the data in the whole time range. However, the index n which is related to the actual dimensionality of the domain growth differs from that predicted with the theory, in the case of heterogeneous nucleation ($n = 2$ for two-dimensional domain growth), indicating slower kinetics of transformation. From optical observation it is clearly seen that the switching processes are initiated with a one-step nucleation and no further domains arise; however, the velocity of the domain walls is not constant during the domain growth. In discussing the experimental data, we assume that TAAP crystal consists of many elementary regions, which have independent switching kinetics. The complex polarization $P(t)$ can be expressed as an integral of the exponential function, equation (1), weighted by a distribution function of characteristic domain growth times $g(\sigma, \tau, t_{0i})$.

$$P(t) = \int g(\sigma, \tau, t_{0i})(1 - \exp[-(t/t_{0i})^n]\mathrm{d}t_{0i}. \tag{2}$$

The distribution of t_0 would, therefore, arise from inhomogeneities in the E_b distribution within the crystal sample. From optical observation of the evolution of the domain structure in this

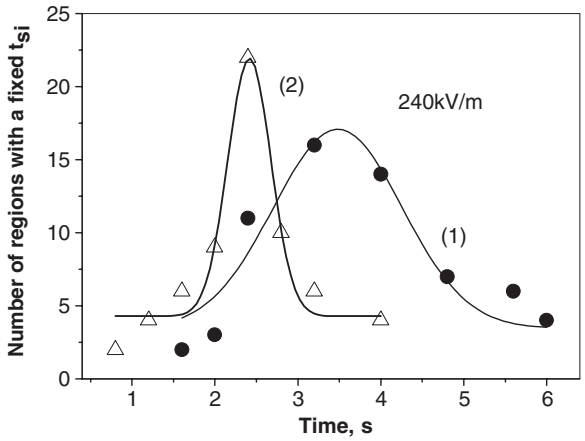

Figure 5. Distribution function of characteristic domain growth times t_s at $E = 240$ kV m^{-1} obtained by measuring the switching time of the elementary regions (symbols) and approximated by a Gaussian function equation (3) (full curves). The switching time was measured in two ways: (1) since the electric field application and (2) from the moment the reversed domain reached the elementary region.

region (as shown in figure 3) it has been found that the spectra of relaxation times can be described by the Gaussian distribution function

$$g(\sigma, \tau, t_{0i}) = \frac{C}{\sqrt{2\pi}\sigma} \exp\left[-\frac{(\tau - t_{0i})^2}{4\sigma^2}\right] \tag{3}$$

with a variance σ. Parameter τ is the averaged characteristic domain growth time and t_{0i} is the characteristic time for the local switching. For this purpose each video frame was divided into 64 square-shaped regions and the switching time of each elementary region was measured until it was covered by the growing domains. The switching time was measured in two ways: (1) since the electric field application and (2) once a domain of reversed polarization reached the elementary region of the crystal. The results obtained for electric field strength of 240 kV m^{-1} are shown in figure 5. The experimental data (symbols) are best approximated by a Gaussian distribution function as given by equation (3). The distribution function of characteristic domain growth times can also be obtained by fitting the experimental data $P(t)$ (as given in figure 4) with a modified KAI function, equation (2), taking σ and τ as variable parameters in the function $g(\sigma, \tau, t_{0i})$ and the value of exponent $n = 2$, which is related to the actual dimensionality of the domain growth. The results are presented in figure 6. There is a good correlation between the distribution function obtained by the fitting procedure (full curves) and that obtained from direct measurement of switching times (broken curves). It must be noted that at $E = 240$ kV m^{-1} the distribution function obtained by the fitting procedure is centred on the averaged characteristic domain growth time $\tau = 2.24$ s, whereas the spectrum obtained by optical observations is centred on the averaged switching time $t_0 = 2.37$ s. Figure 6 presents the latter one after transformation on the time axis. With increasing field E, the spectra of relaxation times move to a shorter τ and become narrower. The distribution of the energy barriers for the domain nucleation determines a broad distribution of the relaxation times. Under applied fields, the relaxation times change. At large enough applied fields the narrow spectrum of short relaxation times is found (figure 6). For higher external fields the domains can switch their orientation more freely since there are fewer obstacles to domain wall motion which can hinder domain switching. The broken curves in figure 4 are the best fit of the

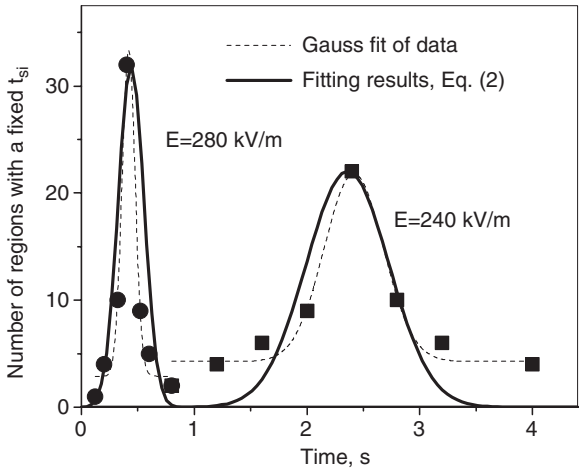

Figure 6. Distribution function of characteristic domain growth times for electric field strength of 240 and 280 kV m^{-1}, obtained by measuring the switching time of the elementary regions (symbols) and derived from the fitting procedure according to equation (2) (full curves). The broken curves correspond to the fit of the data with a Gaussian function given by equation (3).

data with the representation given by equation (3), and the exponent $n = 2$ which represents the behaviour of domain growth. It is worth mentioning that similar Gaussian fittings were obtained for $(CH_3NH_3)_5Bi_2Br_{11}$ crystals [12].

3.2. Kinetics of the switching process in a highly inhomogeneous region of the crystal sample with spatially non-uniform distribution of domain nuclei

The results presented in this section mainly concern the investigation of the influence of inhomogeneities in the internal field distribution on the spontaneous backswitching process. We carried out observation of the domain structure evolution in a highly inhomogeneous fragment of the crystal sample, located in the upper left-hand part of the image in figure 2. Figure 7 shows the series of video frames illustrating the domain pattern evolution during the switching process in $E = 220$ kV m^{-1} (figures 7(a)–(c)) and spontaneous backswitching process after the removal of the electric field (figures 7(d)–(f)). Note that, at $E = 220$ kV m^{-1}, the switching time t_s in which the switched domains grow to fill the whole region (surface area $\sim$1 mm^2) is comparable with t_s measured in the more homogeneous region of the crystal sample at $E =$ 240 kV m^{-1}. There is observed a fast partial switching by nucleation of domains arranged in rows, parallel to the *b*-direction, in the upper part of the image in figure 7(a). The newly formed domains coalesce and then the domain front expands one-dimensionally in the direction nearly perpendicular to the *b*-direction. Further switching continues to occur through nucleation at the domain wall front. At this stage of the switching process, the domain wall velocity and hence the transportation rate shows a marked slowing down. Very approximate estimation gives values from 6×10^{-5} m s^{-1} at the initial stage to 1×10^{-5} m s^{-1} at the end of the switching process. In higher fields, the mechanism of the switching process does not change; only the region with the intensive domain nucleation becomes larger. A similar mechanism of nucleation and growth of domains has been observed during the spontaneous backswitching process. The backswitching process occurs in the reverse order; first nucleation of domains (arranged in chains) are observed in the lower part of the image in figure 7(d). Moreover, generation of

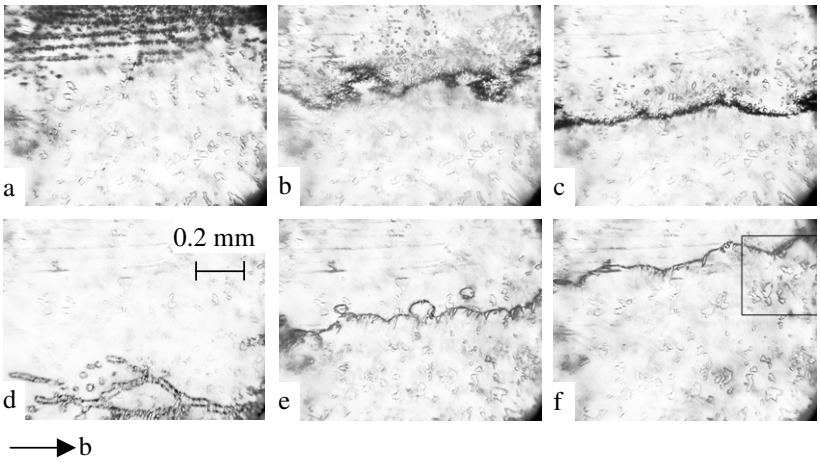

Figure 7. Selected video frames in video recording of domain pattern evolution during switching process in 220 kV m^{-1} (a)–(c) and spontaneous backswitching process after removal of the field (d)–(f). Time from the moment of applying the electric field: (a) 0.1 s (b) 0.6 s (c) 1.2 s. Time from the moment of switching off the electric field: (d) 0.2 s (e) 2.4 s (f) 8 s.

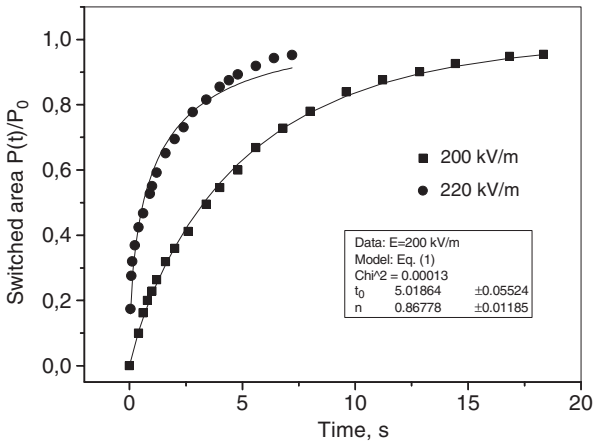

Figure 8. Time dependence of the switched area in electric fields of 200 and 220 kV m^{-1} calculated in a highly inhomogeneous region of the crystal sample.

additional tiny domains in front of the moving domain wall is observed (see figure 7(e)). As we have previously mentioned, the kinetics of switching in such inhomogeneous regions of the crystal sample cannot be analysed on a basis of the KAI model. This is corroborated by figure 8, which plots the fraction of the switched area as a function of time for the evolution of the domain structure as shown in figures 7(a)–(c) (at $E = 220$ kV m^{-1}). Although the full curve, as given by the exponential function, equation (1), corresponds to the best fit of the data for $E = 200$ kV m^{-1}, the resulting growth exponent attains the value $n = 0.86$, and thus differs from that predicted with the KAI model for one-dimensional domain growth ($n = 1$). As was mentioned above, this is brought about by a gradual slowing down of the domain wall velocity.

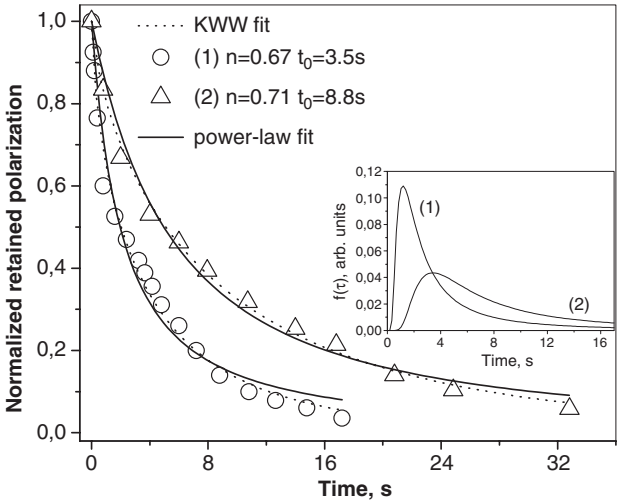

Figure 9. Polarization decay after removal of electric field 200 kV m^{-1} (1) and 220 kV m^{-1} (2) (calculated for domain configuration as shown in figures 7(d)–(f)). The inset shows the distribution functions of relaxation times.

3.2.1. Decay in switchable polarization. The slower kinetics of transformation, of the form $\sim \exp(-t/t_0)^n$ and with exponential coefficient n ranging from 0 to 1, is commonly referred to as stretched exponential decay or termed Kohlrausch–Williams–Watts (KWW) relaxation [29]. This type of relaxation was found to apply not only to ferroelectrics but also to other forms of relaxation, including mechanical, magnetic relaxation, light scattering, and luminescence decay. The existing literature is not consistent regarding their origins and explanations. Thories based on defect diffusion in disordered systems or distribution of relaxation times have been developed [30].

Figure 9 shows the time dependence of normalized retained polarization with respect to the initial polarization $(P_0–P_{(t)})/P_0$ after removal of the poling field of 200 and 220 kV m^{-1} (for domain configuration as shown in figures 7(d)–(f)). The data points are well fitted (broken curves) with a KWW function. The increase in the poling field leads to slowing down of the polarization relaxation, as in higher poling fields the domain structure becomes more stabilized. Direct observation of the domain structure enables us to extract the slowly relaxing component of polarization from the rapid response. In the late-time regime when polarization decay proceeds slowly by the motion of a single domain front, the stretching exponent attains values of 0.53 and 0.48 for plots (1) and (2), respectively. The decrease in n corresponds to a more stretched relaxation and is a reflection of a very broad distribution of relaxation times. Nanoscale investigations using a piezoresponse scanning force microscope have revealed similar polarization decay for PZT family materials [31] and relaxor compound (SBN) [32].

In some disordered ferroelectric crystals the empirical power-law function was used to describe the time-dependent polarization data [33, 34]

$$P(t) = a(1 + t/t_r)^{-n} \tag{4}$$

where t_r is a characteristic relaxation time.

As is shown in figure 9, the experimental data can also be well fitted (full curves) by a power law, equation (4). In this case the polarization has been analysed in terms of polarization relaxation with a distribution of relaxation times, as the mathematical identity of the power-law

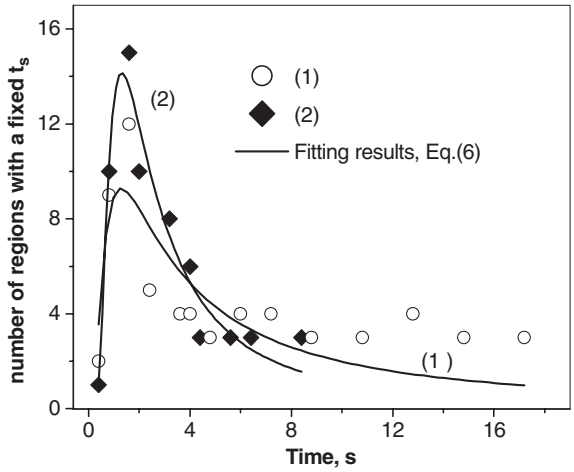

Figure 10. Distribution function of characteristic domain growth times t_s obtained by measuring the polarization reversal time of the elementary regions (symbols) and derived from the fitting procedure, equation (6) (full curves). The time was measured in two ways: (1) once the electric field of 220 kV m^{-1} was removed; (2) from the moment the reversed domain reached the elementary region.

function can be written as [35]

$$P(t) = a(1 + t/t_r)^{-n} = \int_0^\infty f(\tau)\exp(-t/\tau)\mathrm{d}\tau \tag{5}$$

where $\int_0^\infty f(\tau)\mathrm{d}\tau = 1$ is the normalization condition. The distribution function of relaxation times τ satisfying the normalization condition has the form

$$f(\tau) = (t_r\Gamma(n))^{-1}(t_r/\tau)^{n+1}\exp(-t_r/\tau) \tag{6}$$

where $\Gamma(n)$ is the gamma function.

Equation (5) implies that the decay process is a superposition of polarization relaxations with different relaxation times τ. The inset of figure 9 shows the distribution functions of relaxation times $f(\tau)$ deduced from the parameters obtained by fitting the $P(t)$ versus t data to a power law, equation (4). The probable spectrum of the distribution of relaxation times can also be reconstructed from monitoring of the domain pattern, similarly as was described in section 3.1, by measuring the switching time of each (64 elementary areas) small region. As is shown in figure 10, there is a good qualitative agreement between the theoretical predictions $f(\tau)$ (full curves) and the distribution functions obtained by monitoring of the domain structure (given by symbols). It is interesting to note that the polarization decay dynamics described by equation (5) may also represent the averaging of the KAI model over a broad distribution of relaxation times for one-dimensional domain growth (with the exponential coefficient $n = 1$). On analysing the switching process in a more homogeneous fragment of the crystal sample, with a large number of relaxing domains (as shown in figure 3), we obtained a more symmetrical, Gaussian distribution function of characteristic domain growth times.

3.3. Inhomogeneity of internal field distribution

The inhomogeneous distribution of the domain nuclei during switching and spontaneous backswitching processes might be effectively described by the internal bias field E_b, which favours one direction of spontaneous polarization. The domain wall motion can also be affected

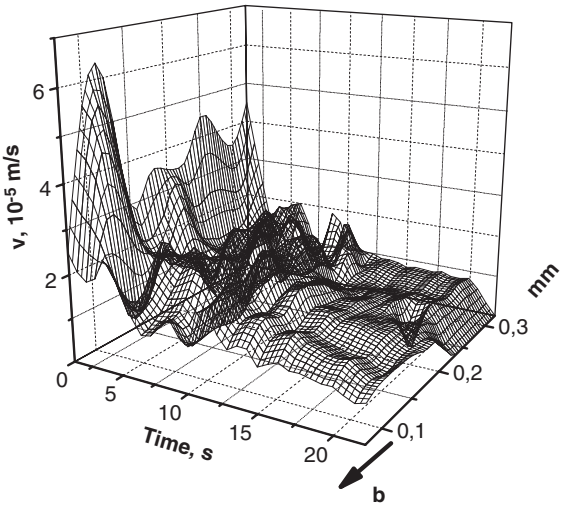

Figure 11. Plot of distribution of velocity corresponding to a domain wall motion during the spontaneous backswitching process (measured in the region set in the frame in figure 7(f)).

by E_b. This can be clearly seen at the last stage of the switching and backswitching processes, where polarization relaxation proceeds by the sidewise motion of the domain wall front. A marked slowing down of the domain wall velocity was observed during its propagation. Such changes of the velocity have originated from the decrease of the effective field, acting on the domain wall. We have presented the real-time kinetics of the domain wall, as shown in figure 7(f), by video imaging with time resolution limited to one frame interval, 40 ms. By arbitrarily assigning a point behind the moving domain wall and by measuring the distance travelled by the domain wall in the propagation direction (normal to the b-direction) we measured the velocity of the wall as a function of the time in this direction. The velocity of domain wall motion was measured at selected points, spaced by 15 μm, located along the b-direction. Figure 11 shows a spatio-temporal distribution of the domain wall velocity calculated for the domain wall movement during the spontaneous backswitching process (see figure 7(f)). The distribution of the domain wall velocity can reflect the non-uniform defect structure distribution within the crystal sample.

In disordered ferroelectric systems, defects locally modify the depth of the double-well potential, giving rise to spatially varying energy barriers for nucleation [28]. The transition from one state to another occurs through the process of the thermal activation type, and the rate for the transition can be described by the expression $\sim \exp(-U/kT)$, where U is the potential barrier against the transition, which is not common for all states of all defects in the crystal. The distribution of potential barriers in energy for the polarized regions determines a broad distribution of the relaxation times. It has been postulated that the sidewise domain growth is a continuous nucleation alongside the existing domain wall [36]. Therefore, it is reasonable to describe the switching process in TAAP crystal by a set of relaxation times. Now it is hard to explain what kind of crystal imperfections or non-uniformities are responsible for stabilization effects and the broad spectrum of potential barriers for the domain walls in TAAP crystal. The volume stabilization of ferroelectric polarization by bulk-ordering of point defect complexes has been shown to be the dominant mechanism in doped [19] and non-stoichiometric [37] crystals. It was reported by Gopalan *et al* [37] that the switching fields in lithium niobate crystals were strongly dependent on the non-stoichiometry. Taking into account the fact that

the TAAP crystal examined has not been defected intentionally, the scale of the backswitching phenomena is surprisingly large. The crystal sample examined was obtained from a non-stoichiometric solution. Thus the origin of E_b in TAAP may be connected with the point defect complexes involving non-stoichiometric defects. During the crystal growth the defects are built in a preferential alignment. They are unable to realign parallel to the new polarization direction. Therefore, after the removal of the poling field, they serve as a source of newly arising domains. A number of regions in TAAP crystal may have different defect concentration than the average as a spatially non-uniform distribution of domain nuclei has been observed during the backswitching process, under the influence of E_b. Additional measurements carried out with some structural studies are needed to ascertain the exact nature of the disorder in TAAP crystal.

4. Conclusions

The results presented provide direct proof of the existence of an in-built internal bias field E_b in a unipolar TAAP crystal sample and that a strong correlation exists between E_b and the domain stabilization mechanism. The internal field caused by structural disorder accounts for the broad spectrum of potential barriers for domain nucleation. Compared with homogeneous TAAP crystal samples the inhomogeneous samples present some characteristic features.

- Non-random distribution of domain nuclei.
- Fluctuation of the single-domain wall velocity by two orders of magnitude.
- In a crystal sample with a large asymmetry of the switching process (the biased field of hysteresis loop E_b is higher than coercive field E_c) the internal field fixes the polarization on the preferred direction strongly, making the new poling state, induced in external field E, unstable. The initial polarization state recovers, at zero E, within a time of milliseconds to several seconds in various regions of the crystal sample.

It has been found that the switching kinetics in TAAP crystal can be approximated by averaging the KAI model over a broad distribution of characteristic domain growth times. The spectra of the relaxation time distribution are drawn from the experimental data.

Acknowledgments

The authors would like to thank Professor Z Czapla from the University of Wrocław for providing the TAAP samples for this study.

References

[1] Scott J F 2006 *J. Phys.: Condens. Matter* **18** R361
[2] Kolmogorov A N 1937 *Izv. Acad. Nauk, Ser. Math.* **3** 355
Avrami M 1940 *J. Chem. Phys.* **8** 212
Ishibashi Y and Takagi Y 1971 *J. Phys. Soc. Japan* **31** 506
[3] Hashimoto S, Orihara H and Ishibashi Y 1994 *J. Phys. Soc. Japan* **63** 1601
[4] Usher T D, Poole C P and Farach H A 1991 *Ferroelectrics* **120** 201
[5] Dimmler K, Parris M, Butter D, Eaton S, Pouligny B, Scott J F and Ishibashi Y 1987 *J. Appl. Phys.* **61** 5467
[6] So Y W, Kim D J, Noh T W, Yoon J-G and Song T K 2005 *Appl. Phys. Lett.* **86** 092905
[7] Kikuta T, Kawagishi Y, El-Maghraby M, Yamazaki T and Nakatani N 2005 *Mater. Sci. Eng.* B **120** 134
[8] Duiker M and Beale P D 1990 *Phys. Rev.* **41** 490
[9] Shur V Ya, Rumyantsev E L and Makarov S D 1998 *J. Appl. Phys.* **84** 445
[10] Jung D J, Dawber M, Scott J F, Sinnamon L J and Gregg J M 2002 *Integr. Ferroelectrics* **48** 59

[11] Tagantsev A K, Stolichnov J, Setter N, Cross S J and Tsukada M 2002 *Phys. Rev.* B **66** 214109
[12] Rogowski R Z, Matyjasek K and Jakubas R 2005 *J. Phys. D: Appl. Phys.* **38** 4145
[13] Wurfel P and Batra I P 1976 *Ferroelectrics* **12** 55
[14] Shur V Y, Rumyantsev E L, Nikolaeva E V, Shishkin E I, Fursov D V, Batchko R G, Eyres L A, Fejer M M and Byer R L 2000 *Appl. Phys. Lett.* **76** 143
[15] Gruverman A and Tanaka M 2001 *J. Appl. Phys.* **89** 1836
[16] Ganpule C S, Roytburd A L, Nagarajan V, Hill B K, Ogale S B, Williams E D, Ramesh R and Scott J F 2001 *Phys. Rev.* B **65** 014101
[17] Stolichnov I, Tagantsev A K, Colla E, Setter N and Cross J S 2005 *J. Appl. Phys.* **98** 084106
[18] Carl K and Hardtl K H 1978 *Ferroelectrics* **17** 473
[19] Lambeck P V and Jonker G H 1986 *J. Phys. Chem. Solids* **47** 453
[20] Robels U, Calderwood J H and Arlt G 1995 *J. Appl. Phys.* **77** 4002
[21] Guo H Y, Xu J B, Xie Z, Luo E Z, Wilson I H and Zhong W L 2002 *Solid State Commun.* **121** 603
[22] Guillot Gauthier S, Peuzin J C, Olivier M and Rolland G 1984 *Ferroelectrics* **52** 293
[23] Gaillard J, Gloux J, Gloux P, Lamotte B and Rius G 1984 *Ferroelectrics* **54** 81
[24] Sobiestianskas R, Grigas J and Czapla Z 1992 *Phase Transit.* **37** 157
[25] Nicolau Y F 1984 *Ferroelectrics* **52** 281
[26] Tikhomirova N A, Dontsova L I, Pikin S A and Shuvalov L A 1979 *JETP Lett.* **29** 34
[27] Matyjasek K and Czapla Z 2000 *Acta Phys. Pol.* A **98** 103
[28] Lines M E and Glass A M 1997 *Principles and Applications of Ferroelectrics and Related Materials* (Oxford: Clarendon)
[29] Kohlrausch R 1854 *Pogg. Ann. Phys.* **91** 56
Williams G and Watts D C 1970 *Trans. Faraday Soc.* **66** 80
[30] Scher M, Shlesinger M F and Bendler J T 1991 *Phys. Today* **44** 26
[31] Gruverman A, Tokumoto H, Prakash A S, Aggarwal S, Yang B, Wutting M, Ramesh R, Auciello O and Venkatesah T 1997 *Appl. Phys. Lett.* **71** 3492
[32] Lehnen P, Kleemann W, Woike Th and Pankrath R 2001 *Phys. Rev.* B **64** 224109
[33] Gladkii V V, Kirikov V A, Nekhlyudov S V and Ivanova E S 2000 *Ferroelectrics* **238** 49
[34] Kang B S, Yoon J G, Noh T W, Song T K, Seo S, Lee Y K and Lee J K 2003 *Appl. Phys. Lett.* **82** 248
[35] Alberici F, Doussineau P and Levelut A 1997 *J. Physique* I **7** 329
[36] Miller R C and Weinreich G 1960 *Phys. Rev.* **117** 1460
[37] Gopalan V, Mitchell T, Furukawa Y and Kitamura K 1998 *Appl. Phys. Lett.* **72** 1981